PROCEEDINGS, 50th Workshop on Geothermal Reservoir Engineering
Stanford University, Stanford, California, February 10-12, 2025
SGP-TR-229

Impacts of Shear Zones on Enhanced Geothermal Systems (EGS): Best Practices for Avoiding Induced Seismicity, Premature Thermal Breakthrough, and Excessive Leakoff

Greg Leveille[1] and Mark D. Zoback[2]

[1] ConocoPhillips (*retired*); currently Tidal Wave Technologies, greg@tidalwavetechnologies.com

[2] Department of Geophysics *Emeritus*, Stanford University, zoback@stanford.edu

Keywords: Enhanced Geothermal Systems, EGS, shear zones, induced seismicity, thermal longevity, fluid leakoff, economic outcomes, horizontal wells, hydraulic fracturing

ABSTRACT

With hydraulically fractured horizontal wells having proven to be an extremely effective method for creating an Enhanced Geothermal System (EGS), we address here questions related to optimizing EGS developments in the context of avoiding negative impacts that can be caused by fluid injection into shear zones. Three questions seem paramount, namely (a) what shear-zone-related attributes threaten the success of an otherwise ideal EGS prospect, (b) how to optimally phase operations to resolve the fundamental challenge of often not knowing if problematic shear-zones exist within a prospective area, and (c) what actions should be taken to mitigate negative economic impacts if problematic zones are encountered. With regard to the first question, when the geothermal community was using hydraulically fractured vertical and moderately-deviated wells for EGS developments, the presence of abundant natural fractures associated with shear zones tended to be seen as a positive attribute. In contrast, it is now clear that shear zones favorably oriented to fail that extend beyond the distance between injectors and producers should not be hydraulically stimulated since the numerous secondary fractures in the damage zones that surround shear zone cores are likely to act as high permeability flow pathways, thereby greatly increasing the risk of induced seismicity, premature thermal breakthrough, and excessive leakoff. Regarding the second question, we recognize that identifying shear zones prior to commencement of development activities can be challenging given the limited ability of current geophysical methods to detect steeply-dipping shear zones in the crystalline basement rocks commonly targeted in EGS developments. Because of this, operations should be phased in such a way that a horizontal well, or preferably a well pair, is drilled and hydraulically fractured during the appraisal phase of a project so that microseismic, fiber optic and other data can be gathered to characterize the interplay between critically stressed shear zones and fluid injection across the intended development area. Doing this will allow operators to attempt to mitigate shear zone related problems by, for example (a) changing where pads are to be placed on the surface and/or the planned location of wells in the subsurface, (b) determining that a certain number of frac stages should be skipped in wells that will intersect shear zones, and (c) refining data gathering strategies so information about the location and nature of shear zones are available before operations get underway on new pads. Encouragingly, when the oil and gas industry has followed a similar phased approach to learning about key geologic uncertainties associated with unconventional reservoir developments, it has generally been able to vastly improve outcomes, suggesting that potentially negative interactions between shear zones and fluid injection can be successfully managed for EGS developments if the right data are acquired early in the life of a project and again before activity expands beyond areas with existing well control.

1. INTRODUCTION

The amount of geothermal energy contained in the Earth's crust that is potentially recoverable is immense, being sufficient to supply all of mankind's primary energy needs for thousands of years (Tester et al., 2006). However, the portion of this energy endowment that has to date been successfully accessed to generate electricity is exceedingly small, with geothermal power today providing less than 0.5% of America's electricity output (EIA, 2024). This disappointing outcome has largely resulted from (a) economically-viable, naturally-occurring hydrothermal systems having proven to be hard to find and/or exploit with technologies used to date, (b) Enhanced Geothermal Systems (EGS) having had a poor track record of delivering economic results (Pollack et al., 2021; Sigfusson and Uihlein, 2015; Breede et al., 2013, Tester et al., 2006), (c) Advanced Geothermal Systems (AGS) being at present technically immature (Blankenship et al., 2024), and (d) large-scale power generation from Hot Sedimentary Aquifers (HSA) having yet to be demonstrated.

Fortunately, the application of a wide range of oilfield technologies to geothermal energy production is poised to enable a dramatic ramp-up in geothermal related power output. This is especially true for EGS, where Utah FORGE and Fervo Energy have demonstrated the ability to markedly reduce the cost of drilling high-angle geothermal wells (Dupriest and Noynaert, 2022; El-Sadi, 2024), and Fervo Energy has established that hydraulically fractured horizontal wells can achieve far higher production rates than the vertical to moderately-deviated EGS wells employed by the geothermal industry since the 1970s (Norbeck and Latimer, 2023; Norbeck et al, 2024).

Given these results, it is worth considering what characteristics an ideal EGS prospect should have when using hydraulically fractured horizontal wells and how this differs from the characteristics historically pursued by EGS operators. In section two of this paper we show that while it was previously believed that prospects with "a high degree of fracturing, high tectonic stresses and low permeability (were) an ideal candidate-EGS reservoir" (Rose et al., 2006; Rose, 2013), when using horizontal wells, it is preferable to avoid highly faulted and tectonically stressed areas, relying instead on multi-stage hydraulic fracturing to create sufficient conductive fracture surface area between injectors and producers. This observation is based on (a) considerable oilfield experience with hydraulically fractured horizontal wells and water disposal related injection, (b) knowledge garnered about the characteristics of basement shear zones from numerous

studies, (c) the production characteristics of fractured basement reservoirs in the Suban gas field in Indonesia, and (d) results of several prior EGS projects that used vertical to near-vertical wells that penetrated shear zones which, when injected into, failed, resulting in large magnitude induced seismic events that shut down the projects (e.g., Basel, Switzerland EGS project, Meier et al., 2015, 2024; and Pohang, Korea EGS development, Ellsworth et al., 2019).

In section three of this paper, we discuss ways to (a) minimize potential problems associated with large-scale shear zones, (b) monitor operations to determine if previously undetected shear zones are present, and (c) mitigate problems that may arise when an EGS development is undertaken in an area containing problematic shear zones. Given the many challenges associated with geophysically resolving shear zones in basement rocks (Eaton et al., 2003), the importance of phasing operations so that microseismicity, fiber optic and other data can be gathered from a hydraulically fractured horizontal well, or preferably a well pair, during the appraisal phase of a project is also covered in section three.

Finally, we offer a series of conclusions and identify areas needing additional study.

2. CHARACTERISTICS OF SHEAR ZONES IMPORTANT TO EGS DEVELOPMENT

2.1 Structural Elements of Shear Zones

Figure 1a (from Johri et al., 2014) shows a generalized morphology of fault zones based on field mapping (Chester and Logan, 1986; Faulkner et al., 2003; Savage and Brodsky, 2011; Gudmundsson, 2022). Two distinct structural elements are shown – the narrow fault core where slip is localized and a much wider damage zone containing numerous macroscopic fractures and faults, extending several tens of meters from the fault core. Because of extensive comminution and the generation of fault gouge, and the mechanical and chemical alteration of the host rock to clay, the fault core may be relatively impermeable with respect to the host rock. The broad damage zone consists of a concentration of small-scale faults that are likely conduits for flow parallel to the main fault trend (Zhang and Sanderson, 1995; Caine et al., 1996a; Paul et al., 2007; Hennings et al., 2012). The Hennings et al. (2012) study in the Suban gas field in South Sumatra is especially noteworthy. As discussed below, tremendous gas flow was channelized along damage zones of large-scale faults located in extremely low permeability granite and dolomite at the edge of a major horst block.

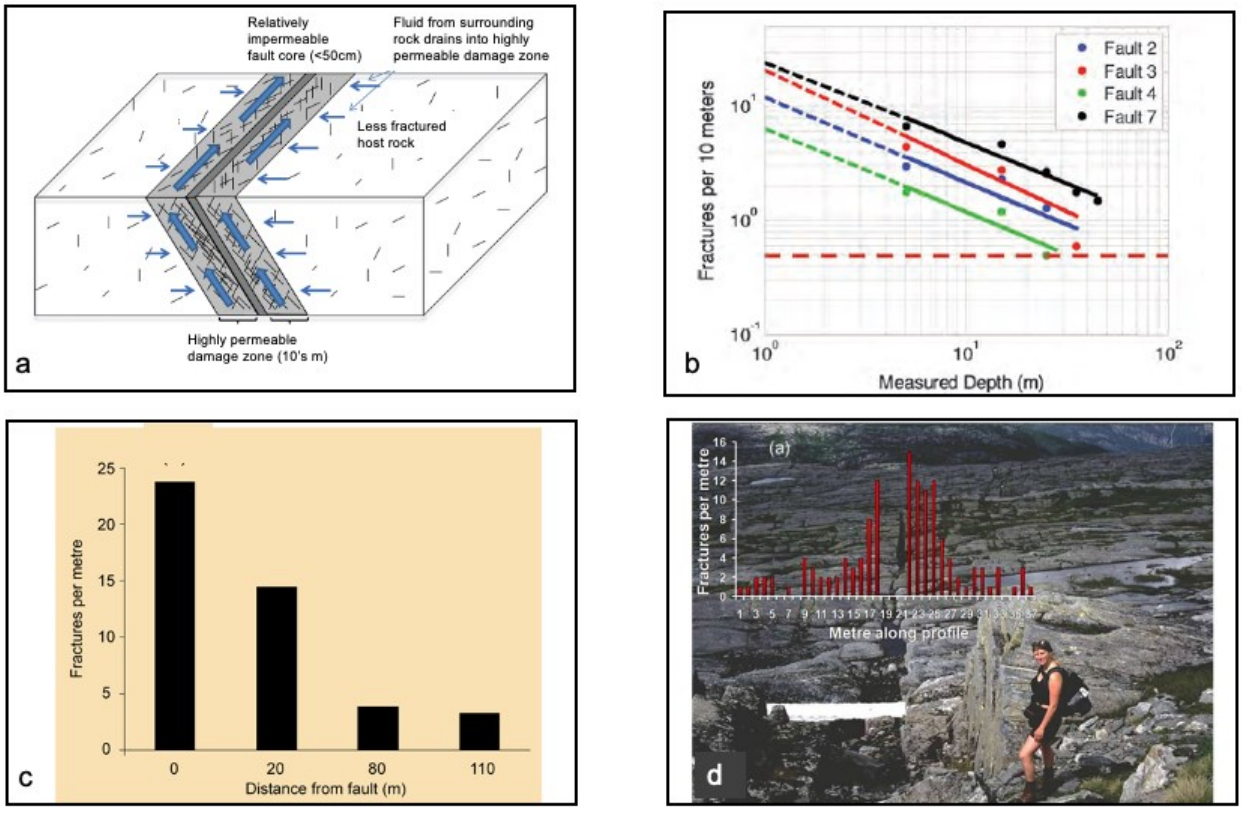

Figure 1: a) A schematic of fault zone structures showing a relatively impermeable fault core surrounded by a highly fractured damage zone. In a fractured, low matrix permeability reservoir, fluid from fractures in the surrounding rock mass drains into the highly permeable damage zones (after Johri et al. 2014). b) Decay of fracture density with distance from faults inside various damage zones encountered in one of the wells in the Suban gas field (after Johri et al. 2014). c) Fracture frequency at specific distances from the core of a large normal fault in west Norway. d) Picture showing how fracture frequency decreases with distance from a small fault in west Norway. The host rock (gneiss) takes over from the damage zone at a distance about 10 m from the fault (from Gudmundsson, 2022).

Figure 1b (from Johri et al., 2014) shows the density of macroscopic fractures (seen in wellbore image logs) from one of the study wells in the Suban field. Note that the fracture density (F) in the damage zone drops off rapidly with distance from the fault (r), reaching the background level of fracture density about 50–80 m from the fault. They found the fracture density to decrease with distance from the fault to follow an exponential decay proposed by Savage and Brodsky (2011) of the form

$$F(r) = F_0 r^{-n}$$

where F_0 is the fracture density at a unit distance from the fault. Interestingly, the value of n found for the damage zones for the faults in this and other Suban wells as well as faults in arkosic sandstone adjacent to the San Andreas fault ranges from about 0.40 to 1.1. These values are generally consistent with the value of 0.8 reported for faults with total slip less than ~150 m by Savage and Brodsky (2011). Perhaps surprisingly, they also found that n decreases for faults with larger displacements. Note that while the degree of fracturing is different for each fault (i.e., F_0 varies from fault to fault) the drop off in fracture frequency (controlled by n) is quite similar and the overall width of the damage zone is many tens of meters.

Figure1c shows fracture frequency at specific distances from the core of a large normal fault in west Norway (from Gudmunson, 2022). Closest to the core/damage zone contact there are 24 fractures per meter, which falls to 14 fractures per meter at 20 m, to 4 fractures per meter at 80 m, and then stays the same to 110 m from the core/damage zone contact, demonstrating how damage zones extend many tens of meters from a fault core. Figure 1d (also from Gudmunson, 2022), demonstrates a similar relationship, a relationship fundamental for understanding why damage zones can significantly augment fluid flow parallel to fault planes.

Utilizing a theoretical model of dynamic rupture along faults analogous to those found in the Suban field, Johri et al. (2014b) showed that the amplified stress magnitudes adjacent to a fault during propagating earthquake ruptures are large enough to break the rock. In fact, their dynamic rupture modeling replicated the drop off in fracture density shown in Figures 1b, 1c and 1d.

2.2 Hydrologic Properties of Shear Zones

Townend and Zoback (2000) summarized observational and modeling data on the bulk hydraulic permeability of upper crustal crystalline basement rocks. They demonstrated that (a) the bulk permeability of crystalline rock, on average, was about 10^{-15} -10^{-16} m^2, about 4 orders-of-magnitude greater than the matrix permeability of the crystalline rocks, (b) the state of stress in the crystalline rocks was in frictional equilibrium, meaning that critically-stressed faults controlled in situ stress magnitudes (*i.e.*, existing faults well-oriented for slip were in a state of incipient frictional failure), and (c) laboratory-derived coefficients of friction of about 0.6 characterized the strength of the crust. Thus, they argued *faulting keeps the crust strong,* meaning that intraplate faults that are currently active in a geologic sense maintain their permeability whereas those that are not seal over time due to precipitation and water rock interaction (*e.g.*, feldspars altering to clays) As shown in Figure 2a, Zoback and Townend (2001) extended the results of Barton et al. (1995) and Townend and Zoback (2000) and showed data from four deep wells that indicated that critically-stressed faults in each well have accentuated permeability compared to faults that are mis-oriented for slip (*i.e.*, mechanically dead faults are also hydraulically dead). Note in the inset of Figure 2 that the ratio of shear to effective normal stress of permeable faults encountered in the four wells peaks at 0.6, the apparent coefficient of friction of critically-stressed faults. Hennings et al., (2012) utilized this concept to investigate the permeability of damage zones in the Suban field mentioned above. The damage zones of these horst-block bounding faults created highly-permeable conduits for natural gas to flow upward from deeper reservoirs in adjacent sedimentary rocks. As shown in Figure 2b, Hennings et al. demonstrated that the number of critically-stressed faults encountered in wells targeted to go through fault damage zones had a remarkable impact on gas production.

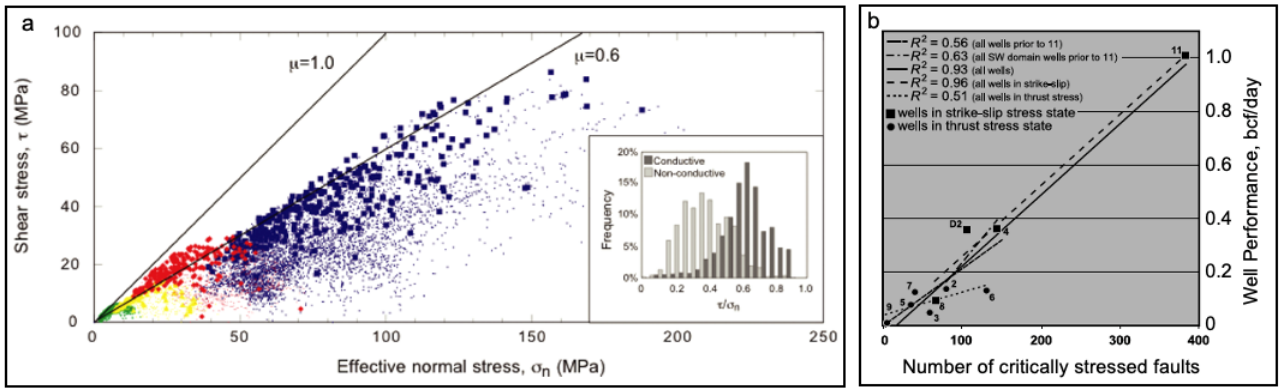

Figure 2: a) Shear and effective normal stress on fractures identified using wellbore imaging techniques in four research wells in crystalline rock (after Zoback and Townend, 2001). The larger filled symbols represent hydraulically conductive fractures as indicated by precise temperature logs. The smaller symbols represent non-conductive fractures. The inset figure illustrates the range of shear to normal stress for all four datasets. b) Flow performance of select well groupings from the Suban field as a function of the number critically-stressed faults encountered (from Hennings et al., 2012).

In the context of geothermal wells encountering faults in crystalline basement rock, the key points are that the damage zones of these faults can extend for tens of meters on either side of the fault core and that these damage zones can be quite permeable, creating the potential for increased risk of elevated levels of induced seismicity, rapid thermal breakthrough, and high levels of injected fluid leakoff.

2.3 Hydraulic Fracturing Induced Seismicity

It is well known that earthquakes induced by hydraulic stimulation have been a major problem for a number of EGS projects. Best known are the cases of the magnitude ~3.5 earthquake associated with the Basel EGS project in Switzerland (Meier et al, 2015; Meier et al., 2024) and the magnitude 5.5 seismic event associated with the Pohong EGS project in South Korea (Figure 3a). It is also well known that horizontal drilling and multi-stage hydraulic fracturing in unconventional reservoirs is sometimes associated with induced seismicity. Figure 3b (after Schultz et al., 2020) is an example from the Eagle Ford shale play in south Texas where hydraulic fracturing induced slip on NE striking normal faults. However, what is particularly relevant for EGS developments but is less widely recognized, is that because crystalline basement rocks are nearly everywhere in a state of incipient frictional failure equilibrium (as discussed in section 2.5 of this paper), the pressure needed to induce slip on critically-stressed basement faults can be very small. This is well illustrated for the case of seismicity associated with the Pohong earthquake. As shown in Figure 3a, seismicity began with the first cycle of injection, continued with increasing maximum magnitudes as subsequent stages were pumped, and ultimately yielded a magnitude 5.5 earthquake, yet the pore pressure changes responsible for triggering the earthquakes were only a few tenths of 1 MPa (Ellsworth et al., 2019).

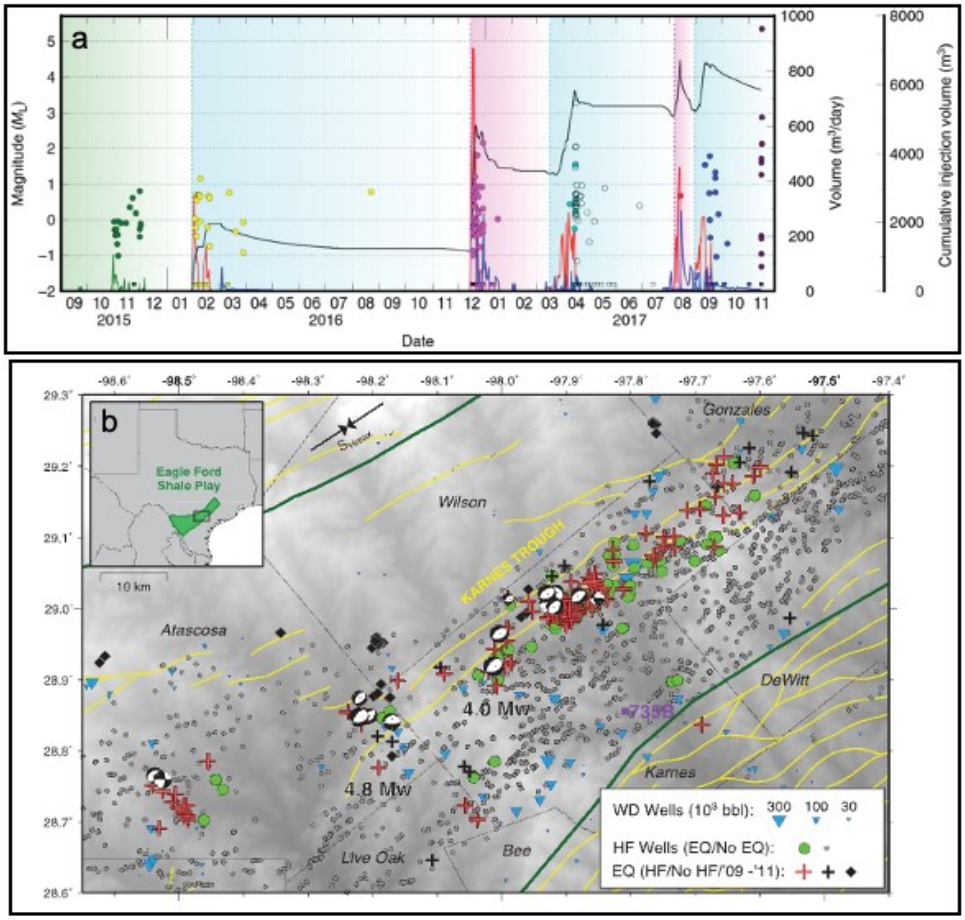

Figure 3: a) Timeline of the Pohang EGS stimulations and seismicity leading up to the 15 November 2017 Mw 5.5 Pohang earthquake (after Ellsworth, et al., 2019). The six shaded periods represent different injection stages. Earthquakes with measured local magnitudes (ML) are represented by colored dots (left scale). Daily injection and flow-back volumes and the cumulative net injection volume are illustrated with colored lines (right scales). b) Locations and timings of Eagle Ford hydraulic fracturing induced seismic events. Map shows earthquakes (crosses) and focal mechanisms (beach balls) since 2017 from the Texas Seismological Network (after Schultz et al., 2020). Correlated earthquakes and hydraulically fractured wells are red and green, respectively. Black diamonds show 2009–2011 earthquakes (Frohlich and Brunt, 2013). Purple square shows the seismic station (735B) used for template matching. Wastewater disposal wells are teal triangles sized by median monthly volumes. Arrows show regional S_{Hmax} orientation (Lund Snee and Zoback, 2022). Faults (after Ewing, 1990) are shown as yellow lines.

In the context of geothermal wells encountering faults in crystalline basement rock, the key points here are that when critically-stressed faults are in the vicinity of wells being hydraulically stimulated, earthquakes can be triggered, even at pressures much less than the least principal stress. The widely recognized fractal nature of earthquake magnitudes distributions is reflected in the observation that for every M 5 earthquake in a region, there are 10 M 4's, 100 M 3's, 1000 M 2's, etc. makes it likely that small earthquakes would be triggered by injection prior to the occurrence of larger magnitude events (as seen in Fig. 3a) because there are so many more small faults than large faults. However, the scaling of earthquake magnitude with injected volume (e.g., Van Der Elst et al., 2016) results from the fact that as more fluid is injected, the probability of encountering a fault capable of triggering relatively larger earthquakes increases.

As discussed below, the Pohong case is quite different from cases such as earthquakes triggered by produced water disposal in Oklahoma, for example. In that case, millions of m^3 were injected in the highly permeable, basal Arbuckle formation (which spread injection-related pressure changes over a very large area) prior to the occurrence of M 5+ earthquakes in underlying crystalline basement rocks. The bottom of the Pohong injection wells were located within 1 km of the fault responsible for the largest earthquakes. Hence, the M 5.5 earthquake occurred at Pohong after injection of only a few thousand m^3 of injection. However, a very important similarity between induced seismicity at Pohong and Oklahoma is that the pressure changes at depth responsible for induced seismicity in Oklahoma also appears to be only about 0.1 MPa at hypocentral depth (Langenbruch et al., 2018).

2.4 Shear Zones Can Hijack Frac Jobs

Another important aspect of permeable fault damage zones is how they can affect hydraulic fracturing operations, as illustrated in Figure 4 from a case study in the Barnett Shale in north Texas. In this case, microseismic events were observed to propagate rapidly along pre-existing faults. The upper part of the figure shows apparent fault zones identified by ant tracking of a post-frac 3D seismic survey. The large apparent northeast trending fault that cuts through the near vertical sections of Wells 1 and 2 is not associated with microseismicity as it was not pressurized. Of particular note are the three northeast trending fault zones labeled A, B and C that cut the horizontal portions of Wells 1 and 2. These are clearly associated with concentrations of microseismic events generated during pressurization of Well 1, as is shown in the lower part of the figure. Note that the microseismic events extend beyond Well 2, apparently due to the high permeability of the damage zones associated with these faults. Of particular interest, the microseismic events along fault C propagated far to the northeast of Well 2 at an azimuth about 25° from that expected for a hydraulic fracture, which is what would be expected for a strike-slip fault, which is not surprising as this is a strike-slip/normal faulting area ($S_V \sim S_{Hmax} > S_{hmin}$). Events along the sub-parallel fault B are also clearly visible that propagate to the southwest from stage 3 in Well 1. In fact, microseismic events occurred along fault C northeast of Well 2 when Well 1 was being stimulated during stages 5 and 6 and pressure was observed to increase in Well 2. More microseismic events along this fault occurred when Well 2 was being stimulated during stages 8–10. All of these observations clearly indicate hydraulic connectivity along fault damage zones from Well 1 to Well 2 and hundreds of meters beyond.

Another way of describing what is seen in Figure 4 is that the pre-existing faults appear to be hijacking a number of the hydraulic fracturing stages, by which we mean that fluid pressure is being diverted along pre-existing fault damage zones. An example of this was presented by Maxwell (2014) where the propagation of microseismic events clearly defines a propagating hydraulic fracture that runs into a pre-existing fault. If this happens relatively close to a well, one would not achieve the intended hydraulic fracture stimulation. Moreover, in the context of geothermal wells, there could be significant leakage of injected fluids well beyond the stimulated wells.

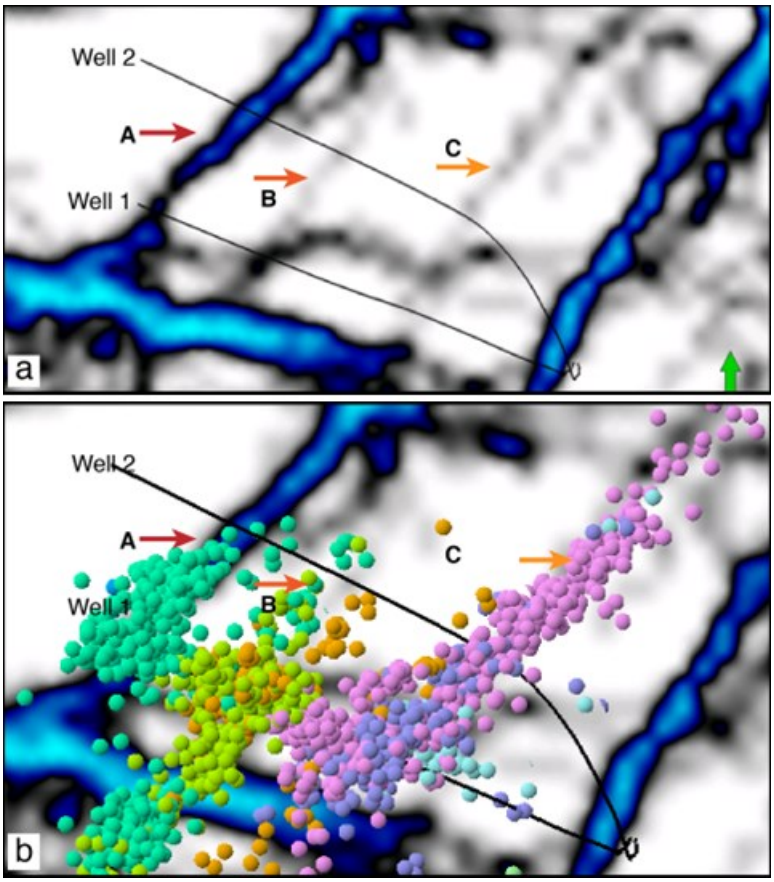

Figure 4: Ant-tracking time slice of a post-frac 3D seismic survey showing apparent faults A, B and C and the association of microseismic events with these faults during hydraulic fracturing in Well 1. Modified after Farghal and Zoback (2016).

2.5 Crystalline Basement Rocks are in Frictional Failure Equilibrium

A critical challenge for geothermal developments in crystalline basement rocks is the abundant evidence that they are in frictional failure equilibrium (Zoback et al., 2002). There are two important implications of this. First, relatively small injection-induced pressure changes are capable of triggering slip on the subset of pre-existing faults in basement that are most well-oriented for slip in the current stress field. This is why the two cases of triggered seismicity cited above, Pohong and Oklahoma, were both caused by pressure changes significantly less than 1 MPa. These are not anomalous cases; they are examples of the fact there are critically-stressed basement faults essentially everywhere. Naturally occurring earthquakes in many intraplate areas slip very infrequently, but even though there is only about 100 years of instrumental seismic monitoring data available, earthquakes have occurred nearly everywhere throughout intraplate regions. This is illustrated by the widespread distribution of seismicity shown in Figure 5 for central and east Asia. The majority of the seismicity is concentrated along major fault zones and regions of high-rate intraplate deformation, such as the Tibetan plateau. This said, many earthquakes occur on more isolated faults, even in relatively quiescent areas such as the Indian shield (shield areas are characterized by stable, cold and thick lithosphere) and eastern China (which is much less seismically active than western China). In these areas note that there are numerous sites of reservoir induced seismicity (red circles) which results from small pore pressure changes at depth resulting from building of dams and impoundment of surface reservoirs. Similar observations have been made in other intraplate areas around the world. Thus, the way to think about the long-term rate of seismicity in an intraplate area is that it reflects the rate at which brittle faulting is occurring in the area, not the stress level.

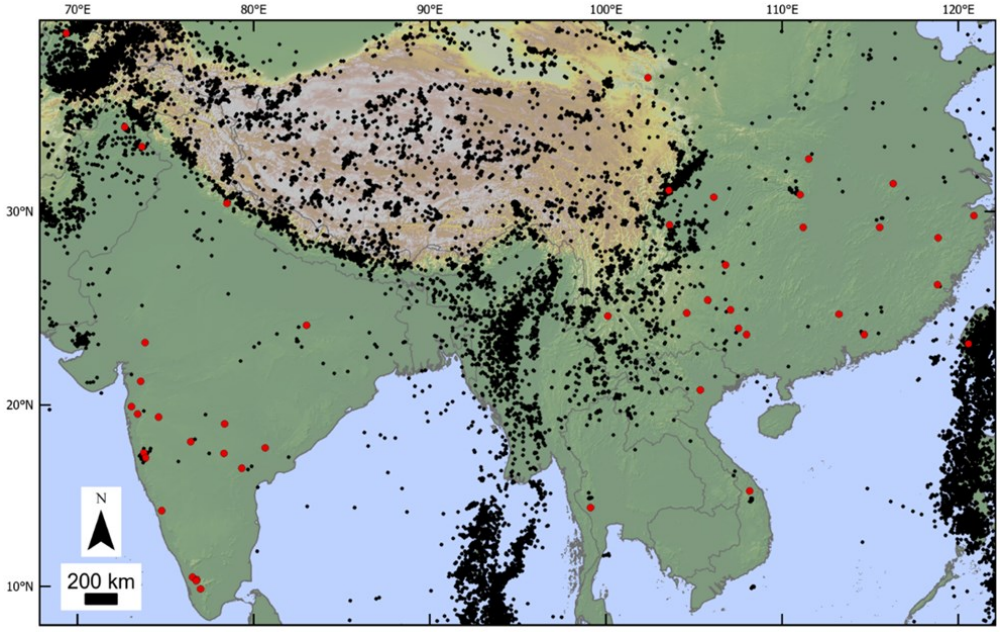

Figure 5. Natural earthquakes (black dots) occurring earthquakes M ≥4.5 since 1970 (U.S. Geological Survey) and sites of seismicity triggered (red dots) by small pressure changes at depth associated with impoundment of reservoirs (Kivi et al., 2023).

Stress magnitudes measured in deep wells and boreholes in crystalline rock confirm that stress levels consistent with Coulomb faulting theory exist everywhere in Earth's crust (e.g., Brudy et al., 1997; Zoback and Harjes, 1997; Lund and Zoback, 1999). Figure 6 (from Townend & Zoback, 2000) summarizes available deep stress measurement in crystalline basin made in different parts of the world. The in-situ stress measurements further show that Coulomb frictional-failure theory incorporating laboratory-derived frictional coefficients, m, of 0.6–1.0 (Byerlee, 1978) gives predictions that are consistent with measured stress states in the upper crust. For instance, at virtually all locations where deep stress levels have been measured, the ratio of the maximum differential stress DS, to the effective mean stress, S– P_p (where S is the mean stress and P_p is the pore pressure), agrees well with that predicted using Coulomb frictional-failure Figure 6 shows that at each of the six locations illustrated, the effective stress data are consistent with values of μ between ~0.6 and 1.0. These data support the hypothesis that the crust contains critically stressed faults that limit its strength. However, because the frictional strength of a faulted rock mass depends on pore pressure, estimates of the frictional strength of the brittle crust depend on the pore pressure at depth. In particular, utilization of Coulomb faulting theory with laboratory-derived coefficients of friction leads to the conclusion that the crust's brittle strength is quite high (hundreds of megapascals) under conditions of approximately hydrostatic pore pressure.

Coulomb faulting theory also predicts the orientation of potentially active faults when the orientation and relative magnitudes of the stress field are known. In simple terms, even if many faults are present, for a coefficient of friction of ~0.6, active normal faults are expected to dip about 60° and strike parallel to the direction of S_{Hmax}. As illustrated by Park et al., (2022), in north-central Oklahoma, strike-slip faults would be expected to be near vertical and strike ±30° to the direction of S_{Hmax}. They showed that fault trends implied by the lineations of seismicity indicate exactly that the great majority of these faults were unknown prior to massive injection of produced water via approximately 800 wells distributed throughout the seismically active area.

The applicability of Coulomb faulting theory means that when a fault is identified, it can easily be determined whether it is potentially active. Walsh and Zoback (2016) demonstrate how this is done while incorporating appropriate uncertainties about the stress state, strike and dip of the fault, etc. In many cases, obtaining prior knowledge of faults in crystalline basement is a difficult thing to determine. The seismicity in north-central Oklahoma resulted from widespread, but quite small (about 1 MPa), pressure increase in the Arbuckle injection zone (Walsh and Zoback, 2015; Langenbruch et al., 2018). In this area, Park et al. located 400,000 earthquakes utilizing advance machine learning and AI techniques. All the earthquakes were in crystalline basement, approximately 5 km below saltwater injection into the Arbuckle. Park et al. also showed that very few of the faults indicated by the seismicity are associated with the faults that were known to exist prior to seismicity induced by massive saltwater disposal.

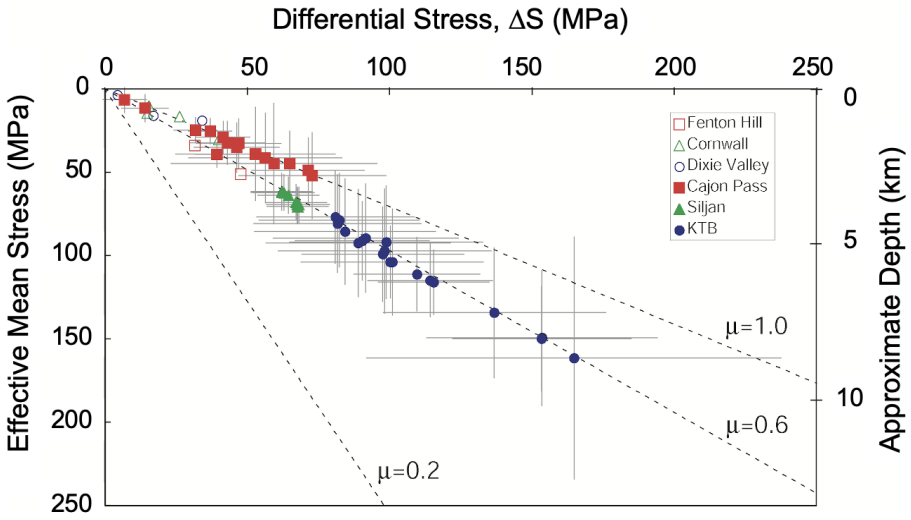

Figure 6: Dependence of differential stress, DS, on effective mean stress, S – Pp, at six locations where deep stress measurements have been made. Dashed lines illustrate relationships predicted using Coulomb frictional failure theory for various coefficients of friction, μ (from Townend and Zoback, 2000).

3. OBVIATING POTENTIAL NEGATIVE IMPACTS OF SHEAR ZONES ON EGS DEVELOPMENTS

3.1 Minimizing the Potential for Problems by Identifying Shear Zones Prior to Drilling

The oil and gas industry has learned that while pre-existing, small-scale fractures can be helpful for increasing recovery from hydraulically stimulated unconventional reservoirs, shear zones that extend beyond the spacing between wells can be problematic since they can hijack frac stages, leading to reduced production, and can act as nucleation sites for induced seismic events sufficiently large to be felt at the Earth's surface, as noted above. That large-scale shear zones can also cause problems for EGS developments is demonstrated by outcomes such as the shear-zone-related induced seismic events triggered by hydraulic fracturing operations in Basel, Switzerland (Meier et al., 2015) and Pohang, Korea (Figure 7), and by the possible hijacking of some of the frac stages at the Utah FORGE test site by preexisting faults (Jurick, 2024). In addition, while not a concern for most unconventional oil and gas reservoirs, for EGS developments, the damage zones of preexisting, large-scale shear zones could easily act as fluid flow superhighways once production commences, as occurs in the fractured-basement-rock-hosted Suban natural gas field in Indonesia, where an absolute open flow rate in excess of one billion cubic feet of gas per day was achieved from a well intersecting a basement shear zone (Koning et al., 2021). In the case of an EGS development, having a fluid flow pathway between injectors and producers along a shear zone with similarly high fluid transmissibility could cause economically crippling levels of premature thermal breakthrough and/or unacceptably high losses of injected fluid. Considerable effort therefore needs to be invested to identify such features during the exploration and appraisal stages of a project.

An example of an EGS project where substantial effort was invested prior to drilling to identify a site devoid of large-scale shear zones is the Haute-Sorne geothermal power project in Switzerland. The site for this development was chosen to maintain a safe distance from faults identified through geophysical surveys and geologic mapping that could present a seismic risk (Meier et al., 2024). Based on oil and gas industry experience, this represents a best practice, a practice that should not only minimize the magnitude of induced seismic events but also lead to better recovery of heat and minimal loss of injected water.

Detecting shear zones in the basement rocks that commonly host geothermal reservoirs prior to drilling can be far more problematic than detecting similar features in sedimentary basins that host oil and gas deposits (Eaton et al., 2003). Because of the high cost of drilling and hydraulically fracturing EGS wells, finding ways to better image structural features within basement rocks deserves considerable attention. Oilfield technologies such as Compressive Seismic Imaging that allow 3D surveys to be acquired at a fraction of the cost of traditional methods (Mosher at al., 2014; Mosher at al., 2017) can undoubtedly help, as can incorporation of rigorous regional geologic mapping into site selection processes (Faulds et al, 2021). However, given the often-significant limitations of currently available techniques for identifying shear zones in basement rocks, monitoring for undetected shear zones during drilling, completion, and production operations is important, as is described in the next section of this paper.

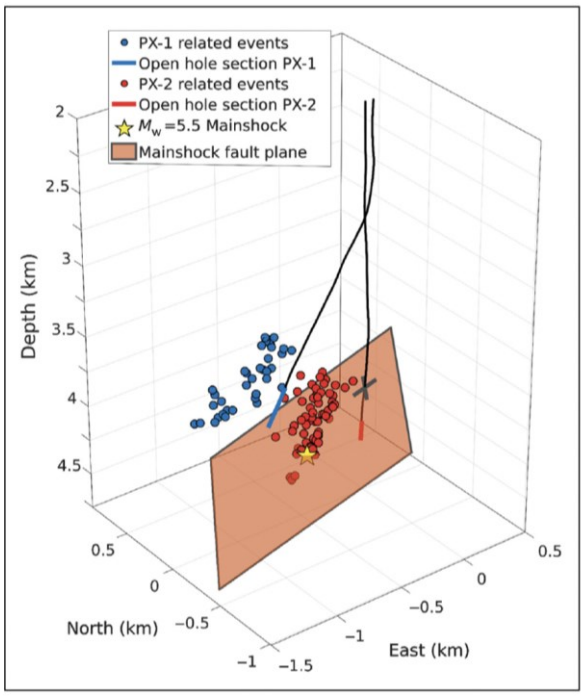

Figure 7: Perspective view of earthquakes induced by attempts to build an EGS injector-producer well pair between the PX-1 (blue) and PX-2 (red) wells, from Ellsworth et al., 2019. The yellow star marks the mainshock hypocenter. Well trajectories are shown with the open-hole sections for PX-1 and PX-2 in blue and red, respectively. The mainshock fault plane intersects PX-2 at 3.8 km depth and is marked by X. As noted in Figure 3, the magnitude of earthquakes escalated during the five different injection periods as the total cumulative volume of injected fluid increased, with the November 2017 magnitude 5.5 event growing outward from its hypocenter beyond the approximately one-kilometer-long segment of the fault that had been activated prior to the event by the stimulations of PX-2 (Ellsworth et al., 2019).

3.2 Monitoring Once Operations are Underway to Determine if Previously Undetected Shear Zones are Present

Given the difficulty of detecting shear zones in basement rocks, monitoring during drilling, completion, and production operations for indications that previously undetected problematic shear zones are present is crucial for optimizing economic outcomes. Oil and gas industry experience indicates this is best done by integrating several types of data, including but not limited to drilling, image log, microseismicity, and fiber optic measurements, with the latter two data types being especially leveraging since they can provide information to help characterize the nature of shear zones at an inter-well-spacing scale.

Seismicity monitoring for the purposes of managing induced seismicity is a relatively mature topic, with protocols having been developed for both EGS and oilfield applications (Majer et al., 2012; Walters et al., 2015; Zoback and Kohli, 2019; Zhou et al., 2024). In general, these protocols emphasize the collection of seismic measurements before, during, and after injection related operations, establishment of "traffic light" seismicity thresholds that if breached require action to be taken to curtail induced seismicity, and community outreach efforts.

Fervo Energy's Cape Project in southwestern Utah provides an example of the effective application of seismicity monitoring and community outreach associated with an EGS development utilizing hydraulically fractured horizontal wells. As reported by Dadi et al. (2024), an extensive microseismic network was deployed at Cape during the stimulation of an initial three wells, with the network comprising shallow borehole sensors, a surface nodal array, deep borehole fiber optic sensors, and three component (3C) passive sensors. During the fracture stimulation operations, a total of five seismic events with magnitudes greater than 2.0 were recorded, necessitating the activation of protocols associated with a pre-determined traffic light system. Injection was paused during three of the five events, with the other two occurring after injection had ceased. Following each amber alert event, seismicity levels returned to normal confirming the effectiveness of the established protocols and response plans (Dadi et al., 2024).

Seismicity monitoring during hydraulic stimulation operations can also be extremely valuable for optimizing EGS developments since microseismicity data can reveal the presence and nature of previously undetected shear zones and/or details about the characteristics of known structural features. Because of this, it will in most cases be beneficial to fracture stimulate a horizontal well, or preferably a well pair, during the appraisal phase of a project to gather microseismicity measurements prior to finalizing pad locations and the layout of development wells. This will allow development wells to be positioned with appropriate standoffs from potentially problematic shear zones that may be present, or when wells must cross structural features, permit operators to plan to skip stages that would otherwise hydraulically stimulate faults and damage zones that would be better left unstimulated, thereby minimizing the risk of induced seismicity greater than the project's traffic light system thresholds, while also improving the probability of thermal longevity and lessening the likelihood of excessive fluid losses.

The value of acquiring high quality microseismic measurements during hydraulic fracturing operations early in the life of an EGS project to not only monitor for and manage induced seismicity but also to detect structural features not identified prior to drilling that could influence project development plans has recently been described by Dadi et al. (2024) for Fervo Energy's Cape Project. At Cape, three of the four horizontal wells that were initially drilled, two of which are planned to be injectors and the other a planned producer, were fracture stimulated a few months apart, with the two injectors being stimulated in mid-February 2024 and the producer in early June. Significant findings derived from the collection of microseismicity data during the stimulation operations that are relevant to the scope of this paper and will undoubtedly be helpful for optimizing the overall Cape development include (a) seismic events tended to be clustered in lineaments trending 10° to 15° NNW-SSE in map view, which was 20° to 30° from the fracture opening direction expected from considerable data indicating S_{Hmax} is locally oriented 10° to 15° NNE-SSW (Figure 8), (b) focal mechanism solutions indicate the dominant failure mode was strike-slip, which suggests shear reactivation occurred on pre-existing faults and fractures, and (c) the data were of sufficient quality that the hydraulic diffusivity of one of the more significant reactivated faults was solved for, yielding insights helpful for understanding the permeability of the feature (Dadi et al., 2024).

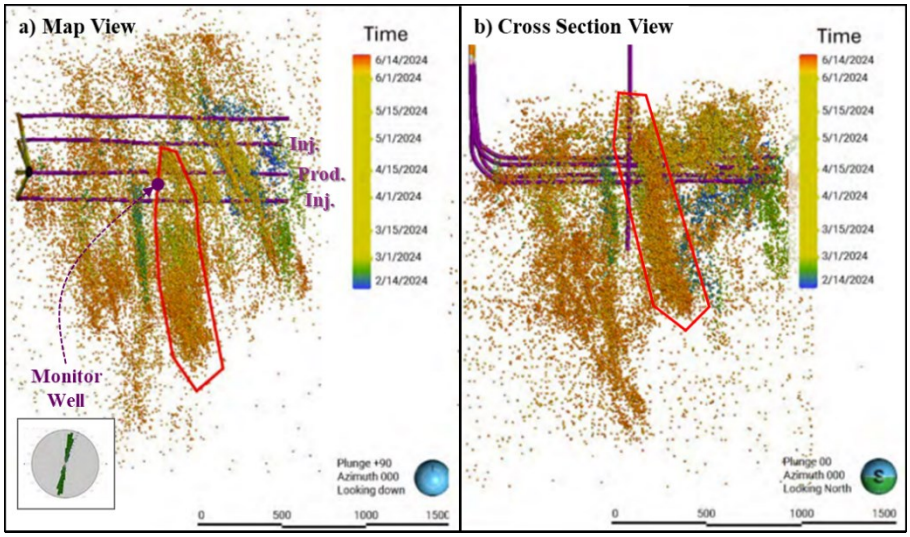

Figure 8: a) Map view of microseismic events recorded during stimulation of two future injection wells (Frisco 1-I and 3-I) and a future production well (Frisco 2-P) at Fervo Energy's Cape Project. The events are color coded as to when they were recorded, with the two injection wells having been stimulated over a three-week period beginning in mid-February 2024, and therefore, are shown as blue, green and yellow dots with the color bar utilized. The production well was fracture stimulated in June 2024, with microseismic events depicted by orange and red dots. Also shown on the map is the location of a vertical monitor well (Delano 1-OB), a rose diagram showing the orientation of drilling induced fractures logged in the monitor well, and a red outline around a collection of seismic events interpreted as resulting from strike-slip reactivation of a preexisting fault for which hydraulic diffusivity calculations were made. b) Cross section view of the same dataset. Figures slightly modified from Dadi et al., 2024.

Oil and gas industry experience and results from the Utah FORGE project has demonstrated that fiber optic measurements (DTS, DAS, DSS) are also a powerful tool for characterizing the nature of fractures extending between wells (Jin and Roy, 2017; Raterman et al., 2019; Jin et al., 2021; Jurick et al., 2025). These types of measurements are especially useful because they can provide not only information about the geometry of fractures extending beyond the distance between wells, and can do so in near real time, but can also qualitatively determine the volume of fluid entering or exiting a well at each perf cluster (depending upon whether a well is a producer or injector), thereby allowing the conductivity of fluid flow pathways to be qualitatively determined. Acquisition of fiber optic datasets early in the life of an EGS project and periodically thereafter is therefore strongly recommended to both identify undetected large-scale shear zones and assess the probability of whether potentially problematic zones pose a significant risk, with the greatest leverage being achieved when these measurements are made in conjunction with the gathering of microseismicity and other complementary datasets (e.g., tracers).

Finally, it needs to be emphasized that monitoring is valuable since it allows for increased understanding, with value being realized by translating understanding into action. This is why deploying a phased data gathering approach is a best practice, with insights garnered from the initial few hydraulically fractured horizontal wells drilled in an area being invaluable for enabling better decisions as long as flexibility has been built into project development plans. Interestingly, having the ability to phase the development of unconventional hydrocarbon reservoirs has added enormous value to these assets compared to originally conceived development plans. Examples of how this can be accomplished for EGS fields are covered in the next section of this paper.

3.3 Mitigating Problems that may Arise when an EGS Development is Undertaken in an Area Containing Shear Zones

When potentially problematic shear zones exist in oil and gas fields being developed using horizontal hydraulically fractured wells, it is common practice to position wells such that horizontal laterals do not intersect the zones, thereby minimizing risks related to induced seismicity, hijacking of frac stages, casing deformation, and poor cement jobs. Or if it is not practical to avoid a shear zone, then operators will skip one or more frac stages to avoid fracing into shear zones that may be critically stressed. These practices also make sense for EGS developments, especially since for EGS projects, possible injection related problems could be encountered not only during hydraulic fracturing operations but also once production commences.

Because EGS developments consist of both production and injection wells, there will be differences in how unconventional reservoir oilfield practices designed to mitigate problems associated with shear zones are applied. For example, in unconventional reservoirs, operators tend to avoid fracture stimulating *all wells* that intersect large-scale shear zones, which is a practice that seemingly would make sense to follow for all EGS *injection wells* since injecting into high permeability shear zones is likely to cause rapid thermal breakthrough, excessive leakoff, and increased risk of large-magnitude induced earthquakes. However, hydraulically fracturing into the same feature in an EGS *production well* will in many cases carry less risk if fluid isn't being injected into the zone once the field comes online, with the upside of such a strategy being that the shear zone might contribute some amount of hydrothermal production, thereby creating a hybrid EGS-hydrothermal system. If this approach is to be followed, it will be important to forego an appropriate number of stages around shear zones in adjacent injectors since the width of damage zones can vary considerably and hybrid-high-permeability-fluid-flow-pathways might be created during hydraulic fracturing operations, as is schematically shown in Figure 9.

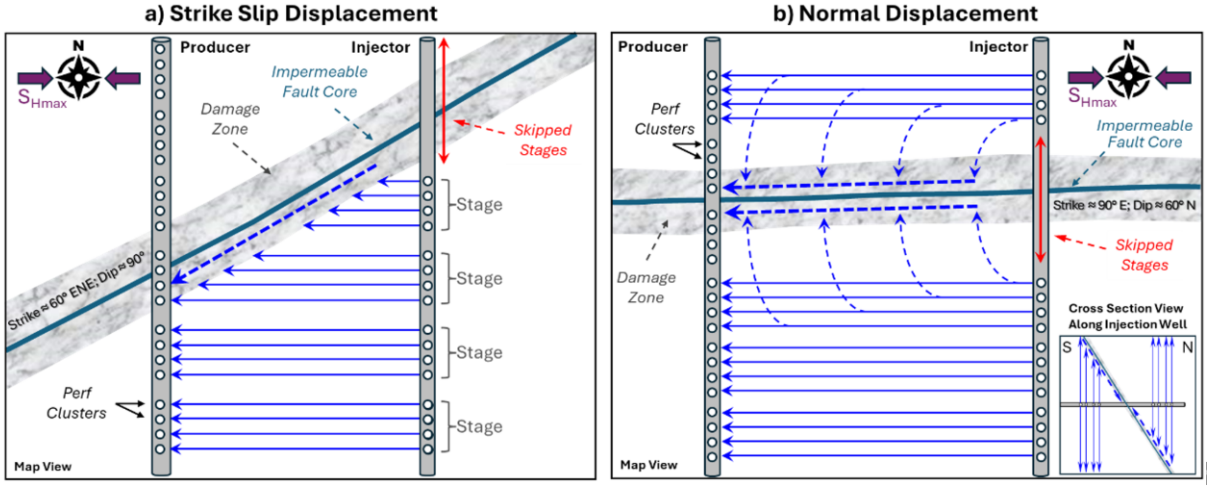

Figure 9: a) Map view depiction of a portion of an EGS injector - producer well pair showing how hybrid fluid flow pathways, that is, pathways that consist of flow through hydraulic fractures for a portion of the distance between the wells and within a pre-existing shear zone for the remainder of the distance, can exist in stress regimes conducive for both normal and strike-slip shearing ($S_v \approx S_{Hmax} > S_{hmin}$). Importantly, the diagram depicts how this can happen even if frac stages are skipped where the injection well intersects the shear zone. Fluid flow in hydraulic fractures is shown by solid blue lines originating from the injection well. Flow in shear zones is shown by dashed lines. Note that hydraulic fractures other than those on the side of the injector facing the production well have been left off to simplify the diagram. b) Map view depiction for a normal fault intersected by an injection – producer well pair in a stress regime where $S_v > S_{Hmax} > S_{hmin}$. By way of explanation about the figure, while the skipped stages eliminate direct fluid flow between the injector and producer, as shown by the cross section in the bottom right corner, given sufficient upward fracture height growth on the south side of the shear zone and downward fracture height growth on the north side, hybrid fluid flow pathways that could cause problems might be created (dashed lines in map view represent flow within the shear zone, not in the plane of the drawing).

The final defense that can be used to try to mitigate injection related problems associated with shear zones consists of either building into the well design the ability to shut-off flow along a portion of a lateral, for example by placing sliding sleeves in the casing string when it is run in the hole, or by attempting to selectively plug off outflow or inflow along portions of a well once problems arise (i.e., depending upon whether it is an injector or producer). Both approaches are extensively utilized to optimize water floods in hydrocarbon reservoirs and manage rising hydrocarbon-water contacts, for example due to water coning. However, because attempts to shut-off unwanted flow paths are often only marginally successful in oil field applications, and because applying these techniques to EGS developments is immature, this is an area deserving considerable additional research and technology development investment.

4. CONCLUSIONS

- Production of electricity from geothermal energy is poised for rapid growth due in part to the transfer of knowledge and technological capabilities developed by the oil and gas industry over the past two decades.
- Knowledge about the structural elements and hydrological properties of shear zones and the fact that crystalline basement rocks are almost everywhere in frictional failure equilibrium will be particularly important for EGS projects.
- Understanding how shear zones are likely to interact with injected fluids is crucial for optimizing EGS developments given the potential negative impacts shear zones can have on thermal longevity, fluid leakoff, and levels of induced seismicity.
- When using hydraulically fractured horizontal wells for EGS developments, it is recommended that extensively faulted and fractured areas – areas that previously were considered attractive EGS targets – be avoided. Instead, operators should rely primarily on multi-stage fracturing to create sufficient conductive fracture surface area between horizontal injectors and producers.
- Fracture stimulating a horizontal well, or preferably a well pair, during the appraisal phase of a project so that microseismicity, fiber optic, tracer, and other complementary measurements can be acquired is an approach that should be considered for all EGS developments since these types of data can identify otherwise hard to detect shear zones and fluid flow pathways, thereby providing information

invaluable for optimizing development plans. For areally large developments, gathering similar information before drilling moves into data sparse portions of the field will allow plans to be adjusted if needed.

- When it comes to mitigating the impacts of potentially problematic shear zones within an EGS development area, a hierarchical approach to minimizing risks, beginning with the most robust risk reduction method, would consist of: (a) placing wells so as to avoid intersecting problematic shear zones, (b) skipping frac stages across and adjacent to shear zones intersected by injectors and producers, (c) skipping frac stages in only the injectors, and (d) relying on zonal shut-off methods to mitigate problems once negative economic impacts are encountered.
- Two areas where additional technology development could greatly improve the ability of operators of EGS developments to manage risks associated with shear zones are: (a) enhancement of geophysical methods that can be used to detect steeply-dipping shear zones in the crystalline basement rocks commonly targeted in EGS developments, and (b) commercialization of zonal shut-off methods robust under the operating conditions encountered in high enthalpy geothermal developments (especially for temperatures in excess of 400 degrees F).
- Finally, it needs to be recognized that while knowledge transfer from the oil and gas industry can help minimize EGS related risks and maximize economic returns, the development of geothermal resources using hydraulically fractured horizontal wells is at present in a nascent stage. By way of demonstrating the truth of this statement, it is worth noting that the number of hydraulically fractured horizontal EGS wells that have been drilled, completed and brought on production is less than 0.005% of the number of such wells deployed to date by the oil and gas industry. There is consequently still much to be learned about how best to utilize hydraulically fractured horizontal wells to produce geothermal energy, which suggests much will be discovered in the years and decades ahead about how shear zone geomechanics impact EGS developments. This causes us to be both excited to see what the future holds and realize that our current state of knowledge is imperfect at best.

5. REFERENCES

Barton, C. A., Zoback, M. D., and Moos, D. (1995). Fluid flow along potentially active faults in crystalline rock. *Geology*, 23(8). doi.org/10.1130/0091-7613(1995)023<0683:FFAPAF>2.3.CO

Blankenship, D., Gertler, C., Kamaludeen, M., O'Connor. M, and Porse, S. (2024). Pathways to Commercial Liftoff: Next-Generation Geothermal Power. *U.S. Department of Energy*.

Breede, K., Dzebisashvili, K., Liu, X., and Falcone, G. (2013). A systematic review of enhanced (or engineered) geothermal systems: past, present and future. *Geothermal Energy*, 1(4). doi.org/10.1186/2195-9706-1-4

Brudy, M., Zoback, M. D., Fuchs, K., Rummel, F., and Baumgärtner, J. (1997). Estimation of the complete stress tensor to 8 km depth in the KTB scientific drill holes: Implications for crustal strength. *Journal of Geophysical Research B: Solid Earth*, 102(B8), 18453-18475. doi.org/10.1029/96JB02942

Caine, J. S., Evans, J. P., & Forster, C. B. (1996). Fault zone architecture and permeability structure. *Geology*, 24(11), 1025. doi.org/10.1130/0091-7613(1996)024<1025:FZAAPS>2.3.CO;2

Chester, F., & Logan, J. (1986). Composite planar fabric of gouge from the Punchbowl Fault, California. *Journal of Structural Geology*, 9(5–6), 621–634. doi.org/10.1016/0191-8141(87)90147-7

Dadi, S., Norbeck, J., Titov, A., Dryer, B., Mohammadi, A., Geng, Y., Obinna, K., Nakata, N., and Matson, G. (2024). Microseismic Monitoring During a Next Generation Enhanced Geothermal System at Cape Modern, Utah. *Geothermal Rising Conference Transactions*, Vol. 48, 1673-1698.

Dupriest, F. and Noynaert, S. (2022). Drilling Practices and Workflows for Geothermal Operations, Paper presented at the *IADC/SPE International Drilling Conference and Exhibition*, Galveston, Texas, USA, March 2022. doi.org/10.2118/208798-M

Eaton, D., Milkereit, B., and Salisbury, M. (editors) (2003). Hardrock Seismic Exploration, *Society of Exploration Geophysicists, Geophysical Development*, No. 10, 277 pages. doi.org/10.1190/1.9781560802396.fm

EIA, 2024, Retail sales of electricity to ultimate customers, *U.S. Energy Information Administration* (EIA) website.

El-Sadi, K., Gierke, B., Howard, E., and Gradl, C. (2024). Review of Drilling Performance in a Horizontal EGS Development, Proceedings, *49th Workshop on Geothermal Reservoir Engineering*, Stanford University, Stanford, California, February 12-14, 2024.

Ellsworth, W. L., Giardini, D., Townend, J., Ge, S., and Shimamoto, T. (2019). Triggering of the Pohang, Korea, Earthquake (M_w 5.5) by Enhanced Geothermal System Stimulation. *Seismological Research Letters*, 90. doi.org/doi: 10.1785/0220190102

Ewing, T. E. (1990). Tectonic map of Texas (scale 1: 750,000). Austin, Texas: *University of Texas Bureau of Economic Geology*.

Farghal, N. S., and Zoback, M. D. (2016). Utilizing ant-tracking to identify slowly slipping faults in the Barnett Shale. Paper presented at the *Unconventional Resources Technology Conference*. doi.org/10.15530/urtec-2014-1922263

Faulds, J, Hinz, N., Coolbaugh, M., Craig, J., Glen, J., Ayling, B., Glen, J., Sadowski, A., Siler, D., and Deoreo, S. (2021). The Nevada geothermal play fairway project: Exploring for blind geothermal systems through integrated geological, geochemical, and geophysical analyses. *Proceedings World Geothermal Congress 2021*, Reykjavik, Iceland.

Faulkner, D. R., Lewis, A. C., and Rutter, E. H. (2003). On the internal structure and mechanics of large strike-slip fault zones: Field observations of the Carboneras fault in southeastern Spain. *Tectonophysics*, 367(3–4), 235–251. doi.org/10.1016/S0040-1951(03)00134-3

Frohlich, C., and Brunt, M. (2013). Two-year survey of earthquakes and injection/production wells in the Eagle Ford Shale, Texas, prior to the Mw 4.8 20 October 2011 earthquake. *Earth and Planetary Science Letters*, 379, 56–63. doi.org/10.1016/j.epsl.2013.07.025

Gudmundsson, A. (2022). Transport of Geothermal Fluids along Dikes and Fault Zones. *Energies*, 15(19), 7106. doi.org/10.3390/en15197106

Hennings, P., Allwardt, P., Paul, P., Zahm, C., Reid, R., and Alley, H. (2012). Relationship between fractures, fault zones, stress, and reservoir productivity in the Suban gas field, Sumatra, Indonesia. *AAPG Bulletin*, 96(4), 753–772. doi.org/10.1306/08161109084

Jin, G. and Roy, B. (2017). Hydraulic-fracture geometry characterization using low-frequency DAS signal. *Leading Edge*, Volume 36(12), 975–980. doi.org/10.1190/tle36120975.1

Jin, G., Ugueto, G., Wojtaszek, M., Guzik, A., Jurick, D., and Kishida, K. (2021). Novel Near-Wellbore Fracture Diagnosis for Unconventional Wells Using High-Resolution Distributed Strain Sensing during Production. *SPE Journal*, 26(05), 3255–3264. SPE-205394-PA. doi.org/10.2118/205394-PA

Johri, M., Zoback, M. D., and Hennings, P. (2014). A scaling law to characterize fault-damage zones at reservoir depths. *AAPG Bulletin*, 98(10), 2057–2079. doi.org/10.1306/05061413173

Jurick, D. (2024). Utah FORGE Distributed Fiber Optic Sensing: Introduction and Overview of Results. [Online] *Utah FORGE Research News Webinar*. https://utahforge.com/2024/10/17/webinar-series-featuring-d-jurick-of-neubrex/

Jurick, D., Reynolds, A. and Sharma, M. (2025). Improving the Connectivity between Injection and Production Wells in Enhanced Geothermal Systems Using Fiber Optic Data. SPE *Hydraulic Fracturing Technology Conference and Exhibition*, SPE-223456-MS.

Kivi, I. R., Boyet, A., Wu, H., Walter, L., Hanson-Hedgecock, S., Parisio, F., and Vilarrasa, V. (2023). Global physics-based database of injection-induced seismicity. *Earth System Science Data*, 15(7), 3163–3182. doi.org/10.5194/essd-15-3163-2023

Koning, T., Cameron, N., and Clure, J. (2021). Undiscovered Hydrocarbon Potential in Sumatra. [Online] *GeoExPro*. https://geoexpro.com/undiscovered-hydrocarbon-potential-in-sumatra/

Langenbruch, C., Weingarten, M., and Zoback, M. D. (2018). Physics-based forecasting of man-made earthquake hazards in Oklahoma and Kansas. *Nature Communications*, 9(1), 3946. doi.org/10.1038/s41467-018-06167-4

Lund, B., and Zoback, M. D. (1999). Orientation and magnitude of in situ stress to 6.5 km depth in the Baltic Shield. *International Journal of Rock Mechanics and Mining Sciences*, 36(2). doi.org/10.1016/S0148-9062(98)00183-1

Lund Snee, J.-E., and Zoback, M. D. (2022). State of stress in areas of active unconventional oil and gas development in North America. *AAPG Bulletin*, 106(2), 355–385. doi.org/10.1306/08102120151

Majer, E., Nelson, J., Robertson-Tait, A., Savy, J., and Wong, I. (2012). Protocol for Addressing Induced Seismicity Associated with Enhanced Geothermal Systems. *US Department of Energy Geothermal Technologies Office*, DOE/EE-0662.

Marsh, S. and Holland, A. (2016). Comprehensive Fault Database and Interpretive Fault Map of Oklahoma. *Oklahoma Geological Survey Open-File Report* (OF2-2016), 15.

Maxwell, S. C. (2014). Microseismic Imaging of Hydraulic Fracturing: Improved Engineering of Unconventional Shale Reservoirs. *Society of Exploration Geophysicists*. doi.org/10.1190/1.9781560803164

Meier, P., Alcolea Rodríguez, A., Bethmann, F. (2015). Lessons learnt from Basel: New EGS projects in Switzerland using multistage stimulation and a probabilistic traffic light system for the reduction of seismic risk. *Proceedings World Geothermal Congress 2015*, Melbourne, Australia, 19-25 April 2015.

Meier, P., Zingg, O., Alcolea Rodríguez, A., Bethmann, F., Dyer, B., Karvounis, D., Ollinger, D., Fiori, R., and Serbeto, F. (2024). Learning curve of seismic risk mitigation for EGS since Basel 2006 to Utah FORGE 2024 from the perspective of a project developer. Paper presented at the *Geothermal Rising Conference*, Waikoloa, Hawaii, October 10, 2024.

Mosher, C., Li, C., Morley, L., Ji, Y., Janiszewski, F., Olson, R., and Brewer, J. (2014). Increasing the efficiency of seismic data acquisition via compressive sensing. *The Leading Edge*, 33, pages 386–388, 390–391. doi.org/10.1190/tle33040386.1

Mosher, C., Li, C., Ji, Y., Janiszewski, F., Bankhead, B., Williams, L., Hand, J., and Anderson, J. (2017). Compressive Seismic Imaging: Moving from research to production. Paper presented at the 2017 *SEG International Exposition and Annual Meeting*, Houston, Texas, September 2017. SEG-2017-17679803

Norbeck, J., and Latimer, T. (2023). Commercial-scale demonstration of a first-of-a-kind Enhanced Geothermal System. *EarthArXiv*. doi.org/10.31223/X52X0B

Norbeck, J., Gradl, C., and Latimer, T. (2024). Deployment of Enhanced Geothermal System technology leads to rapid cost reductions and performance improvements. *EarthArXiv*. doi.org/10.31223/X5VH8C

Park, Y., Beroza, G. C., and Ellsworth, W. L. (2022). Basement Fault Activation before Larger Earthquakes in Oklahoma and Kansas. *The Seismic Record*, 2(3), 197–206. doi.org/10.1785/0320220020

Paul, P., Zoback, M., and Hennings, P. (2007). Fluid flow in a fractured reservoir using a geomechanically-constrained fault zone damage model for reservoir simulation. In Proceedings - *SPE Annual Technical Conference and Exhibition* (Vol. 5).

Pollack, A., Horne, R., and Mukerji, T. (2021). What Are the Challenges in Developing Enhanced Geothermal Systems (EGS)? Observations from 64 EGS Sites. *Proceedings World Geothermal Congress*, Reykjavik, Iceland.

Raterman, K., Liu, Y. and Warren, L. (2019). Analysis of a Drained Rock Volume: An Eagle Ford Example. Paper presented at the SPE/AAPG/SEG *Unconventional Resources Technology Conference*. doi.org/10.15530/urtec-2019-263

Rose, P. (2013). Creation of an Enhanced Geothermal System through Hydraulic and Thermal Stimulation, Final Report. *Energy and Geoscience Institute at the University of Utah*, Contract DE-FC07-01ID14186. doi.org/10.2172/1076593

Rose, P., Hickman, S., McCulloch, J., Davatzes, N., Moore, J., Kovac, K., Adams, M., Mella, M., Wannamaker, P., Julian, B., Foulger, G., Swenson, D., Gosavi, S., Bhat, A., Richards-Dinger, K., Monastero, F., Weidler, R., Baisch, S., Ghassemi, A., Kohl, T. and Megel, T. (2006). Final Report for the Portion of the Project Focused on the East Compartment of the Coso Geothermal Field, Volume 1, Creation of an Enhanced Geothermal System through Hydraulic and Thermal Stimulation. *Energy and Geoscience* Institute at the University of Utah, Contract DE-FC07-01ID14186.

Paul, P., Zoback, M., and Hennings, P. (2007). Fluid flow in a fractured reservoir using a geomechanically-constrained fault zone damage model for reservoir simulation. In Proceedings - *SPE Annual Technical Conference and Exhibition* (Vol. 5).

Savage, H. M., & Brodsky, E. E. (2011). Collateral damage: Evolution with displacement of fracture distribution and secondary fault strands in fault damage zones. *Journal of Geophysical Research*, 116(B3), B03405. doi.org/10.1029/2010JB007665

Schultz, R., Skoumal, R. J., Brudzinski, M. R., Eaton, D., Baptie, B., & Ellsworth, W. (2020). Hydraulic Fracturing-Induced Seismicity. *Reviews of Geophysics*, 58(3), e2019RG000695. doi.org/10.1029/2019RG000695

Townend, J., & Zoback, M. D. (2000). How faulting keeps the crust strong. *Geology*, 28(5), 399-402. https://doi.org/10.1130/0091-7613(2000)28<399:HFKTCS>2.0.CO;2

Van Der Elst, N. J., Page, M. T., Weiser, D. A., Goebel, T. H. W., & Hosseini, S. M. (2016). Induced earthquake magnitudes are as large as (statistically) expected. *Journal of Geophysical Research: Solid Earth*, 121(6), 4575–4590. doi.org/10.1002/2016JB012818

Walsh, F. R., & Zoback, M. D. (2015). Oklahoma's recent earthquakes and saltwater disposal. *Science Advances*, 1(5). doi.org/10.1126/sciadv.1500195

Walsh, F. R., & Zoback, M. D. (2016). Probabilistic assessment of potential fault slip related to injection induced earthquakes: Application to north-central Oklahoma, USA. *Geology*, 44(12). doi.org/10.1130/G38275.1

Zhang, X., & Sanderson, D. J. (1995). Anisotropic features of geometry and permeability in fractured rock masses. *Engineering Geology*, 40(1–2), 65–75. doi.org/10.1016/0013-7952(95)00040-2

Zhou, W., Lanza, F., Grigoratos, I., Schultz, R., Cousse, J., Trutnevyte, E., Muntendam-Bos, A. and Wiemer, S. (2024). Managing induced seismicity risks from enhanced geothermal systems: A good practice guideline. *Reviews of Geophysics*, 62, doi.org/10.1029/2024RG000849

Zoback, M. D., & Townend, J. (2001). Implications of hydrostatic pore pressures and high crustal strength for the deformation of intraplate lithosphere. *Tectonophysics*, 336(1–4). doi.org/10.1016/S0040-1951(01)00091-9

Zoback, M. D., Townend, J., & Grollimund, B. (2002). Steady-state failure equilibrium and deformation of intraplate lithosphere. *International Geology Review*, 44(5). doi.org/10.2747/0020-6814.44.5.383